Thermo-Optical Enhanced Silicon Wire Interleavers

J. F. Song, S. H. Tao, Q. Fang, T. Y. Liow, M. B. Yu, G. Q. Lo, and D. L. Kwong

***Abstract*—Ring-resonator (RR) and ring-assisted (RA) Mach–Zehnder interferometer (MZI) interleaver structures with thermo-optical fine tuning are proposed and fabricated on silicon-on-insulator. With thermo-optical fine tuning, the crosstalks are improved from ∼12 to ∼22 dB and from ∼6 to ∼17 dB for RR- and RA-MZI interleavers, respectively. In a wavelength range of 40 nm, the RR-MZI interleaver structure has more uniform responses whereas the RA-MZI interleaver structure has sharper rolloffs.**

***Index Terms*—Integrated optics, optical communication, silicon-on-insulator, thermo-optics effect, waveguide filters.**

I. Introduction

INTERLEAVER structure is one of the key devices in future dense wavelength-division-multiplexing applications [1]–[3]. Many optical filters have been investigated [4]. Interleavers were designed and implemented in many varieties, such as the Michelson–Gires–Tournois interferometer (MGTI) [5], [6], bulk birefringent crystals [7], [8], fibers [9]–[11], and the planar-lightwave circuits (PLCs) [12]–[20]. Among these, the structures of MGTI, the bulk birefringent crystals, and the fibers cannot be integrated with other devices on a chip. On the contrary, the PLC devices are attractive for being compact, cost-effective, and compatible with standard complementary metal–oxide–semiconductor technology. Wörhoff *et al.* [17] reported a crosstalk of ∼14 dB in a 2×2 ring-assisted Mach–Zehnder interferometer (RA-MZI) structure on SiON with thermo-optical effect utilized. Low polarization dependence was also achieved. Wang *et al.* [18] reported a SiO_2-based double-ring MZI structure and obtained a crosstalk of ∼30 dB. In our recent work [19], [20], two 1×2 interleaver structures were designed and fabricated on 300 nm × 300 nm silicon wire waveguide. Reference [19] is a compact ring-resonator Mach-Zehnder interferometer (RR-MZI) structure, which comprises a ring resonator (RR) and a 3-dB directional coupler (DC). Reference [20] is a Y-branch RA-MZI structure, which has an RR coupled with one arm-waveguide in the 1×2 MZI structure. About 10-dB crosstalk was achieved in both structures. Due to inevitable process variations from fabrication, it is difficult to improve the crosstalk by implementing passive devices alone.

Manuscript received July 03, 2008; revised September 22, 2008. First published October 31, 2008; current version published December 12, 2008.

J. F. Song is with the Institute of Microelectronics, A*STAR, Singapore 117685, Singapore, and also with the State Key Laboratory on Integrated Opto-Electronics, College of Electronic Science and Engineering, Jilin University, Changchun 130023, China (e-mail: songjf@ime.a-star.edu.sg).

S. H. Tao, Q. Fang, T. Y. Liow, M. B. Yu, G. Q. Lo, and D. L. Kwong are with the Institute of Microelectronics, A*STAR, Singapore 117685, Singapore.

Color versions of one or more of the figures in this letter are available online at http://ieeexplore.ieee.org.

Digital Object Identifier 10.1109/LPT.2008.2007572

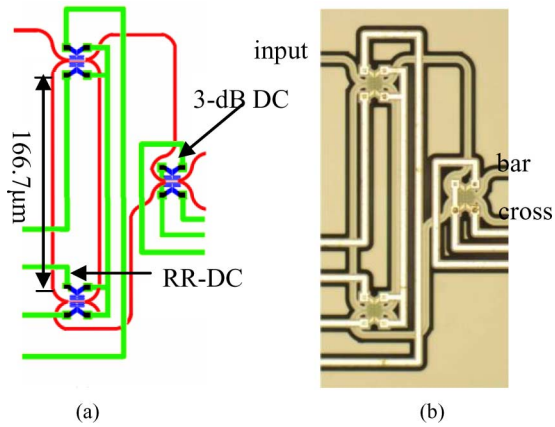

Fig. 1. (a) Layout of the full RR-MZI interleaver structure. The red curve is the silicon waveguide and the blue curve is the Ti heater. The green line is the aluminum. (b) Microscope picture of the full RR-MZI interleaver structure, where the dark regions are deep trenches.

In this letter, we replace the 300 nm × 300 nm silicon wires with 400 nm × 200 nm ones. Although it is difficult to obtain negligible birefringence for an RR with long perimeter, the loss of transverse-electric (TE) mode in 400 nm × 200 nm silicon waveguides would be lower, and the thermo-optical fine tuning can be explored to improve the crosstalk performance. In this study, we will investigate the RR- and RA-MZI devices.

II. Fabrication

We started the fabrication on a 200-mm silicon-on-insulator wafer with 400-nm-thick top silicon and 2-μm-thick buried oxide (BOX). The top silicon was thinned down to 200 nm by thermal oxidation. First, 50-nm undoped silicate glass oxide was deposited as hard mask. The 248-nm-deep UV lithography was used to define the device pattern, and the inductively coupled plasma etching system was used to dry etch the hard mask layer. The pattern of the hard mask was then transferred to form the device structure. The Si layer was dry etched until the BOX layer was exposed. Spot size converters (SSCs) were integrated for the input and output terminals. The SSC is a 200-μm-long taper with 200-nm tip width.

The waveguide of the RR-MZI interleaver is illustrated in Fig. 1(a) (red line). The length of the 3-dB DC is 11 μm and the gap of two waveguides is 0.3 μm. The length of the RR-DC is 14.5 μm and the gap is also 0.3 μm.

After deposition of 1-μm high-density plasma (HDP) oxide, 100-nm titanium (Ti) was deposited. Ti was chosen as the heater metal for its high electrical and heat resistances. The

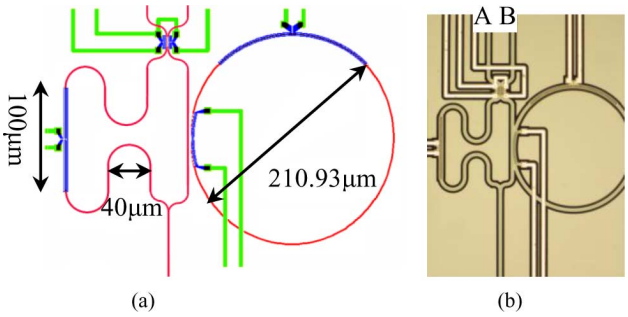

Fig. 2. (a) Layout of the full RA-MZI interleaver structure. The red curve is the silicon waveguide and the blue curve is the Ti heater. The green line is the aluminum. (b) Microscope picture of the full RA-MZI interleaver structure.

UV lithography was applied to define the heater pattern. The heater was etched as a saw-like shape to increase the electrical resistance. The heaters are shown as a blue curve in Fig. 1(a). Both the width of the Ti wire and the gap between the wires are 500 nm. The total length of the Ti strip is ∼60 μm. Then, 1-μm HDP oxide was deposited again. After the formation of contact holes, 750-nm aluminum was deposited shown as a green line in Fig. 1(a). The final process was the deep trenches etch. The deep trench is a 3-μm-wide groove. The groove edge is 3 μm away from the waveguide and 2 μm away from the metal (heat or pad). The deep trench will be used to prevent heat diffusion. The depth of the groove is ∼100 μm. Besides for the heat isolation, the groove is also used for easier fiber coupling. The tip of the enclosed SSC is 3 μm away from the coupling facet. The final device is shown in Fig. 1(b), where the dark regions are the deep etched grooves. The total length of the device is 2.9 mm.

An RA-MZI interleaver was fabricated at the same time. The layout is shown in Fig. 2(a). The structure parameters of the 3-dB DC are the same as those of the RR-MZI interleaver, in which a delay line is incorporated in one arm of the MZI and an RR is coupled with the other arm. The diameter of the ring is 210.93 μm. The final device is shown in Fig. 2(b).

III. Results and Discussion

During the measurements, the insertion loss (IL) was recorded as the fiber-to-fiber loss, which included the device transmission loss and the coupling loss between a fiber and an SSC. Two lensed polarization-maintaining fibers were coupled with the input and the output silicon wires, respectively. We used a polarization controller to choose a quasi-TE mode (electric field parallel to the substrate plane) from an amplified spontaneous emission light source. We connected the broadband light source, the polarization controller, and an optical spectrum analyzer with polarization-maintaining fibers, and then measured the IL at TE polarization, which was set by the polarization controller. The measured polarization controller's IL was used as reference for the subsequent measurements. Then, we deducted the reference IL from the subsequent IL measurements.

First, we characterized the 1×2 RR-MZI interleaver. Fig. 3(a) presents IL spectra of the bar and the cross waveguides. The wavelength is from 1550 to 1590 nm. The measured

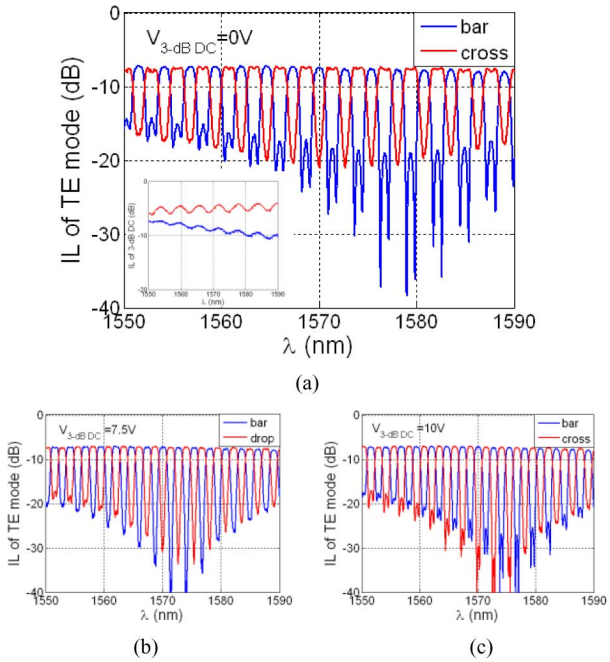

Fig. 3. Spectra of the 1×2 RR-MZI interleaver. (a) Spectra of the bar and the cross waveguides of the RR-MZI with 0 V on the 3-dB DC. The inset is the spectra of the 3-dB DC. (b) Spectra of the bar and the cross waveguides of the RR-MZI with 7.5 V applied. (c) Spectra of the bar and the cross waveguides of the RR-MZI with 10 V applied.

crosstalk is ∼10 dB. Although the crosstalk is almost the same as our recent results [19], we have not yet applied any voltage on the heater beneath the 3-dB DC. For reference, spectra of a separate 3-dB DC are inserted. Due to fabrication variation, it is difficult to evenly split light in two terminals exactly as designed. For our case, the optical power in the cross terminal is higher than that of the bar. Fig. 3(b) is the response spectra of the RR-MZI interleaver applied with 7.5 V (∼25.5 mW). At ∼1570 nm, the crosstalk is improved from ∼12 to ∼22 dB, by almost ∼10 dB. If the electric voltage is increased to 10 V (∼45 mW), the spectrum will split into two "grooves" in the bottom and the crosstalk will not be further improved. Two factors might induce the split "grooves" in the spectrum of the RR-MZI. One is the loss of the RR and the other is the uneven light powers in the outputs of the 3-dB DC. As the responses of the interleaver are very sensitive to the outputs of the 3-dB DC, the lights in the bar and the cross waveguides can be balanced by tuning the 3-dB DC. The profile of the response spectrum is also dependent on wavelength.

Similarly, the responses from a 1×2 RA-MZI interleaver structure are shown in Fig. 4(a) and (b). Without tuning, the crosstalk is only ∼6 dB. Once we applied a bias of 11 V (∼51.4 mW) on the 3-dB DC, the crosstalk was found to be improved to ∼17 dB.

The passbands of both the structures are shown in Fig. 5, in which the output powers have been normalized. We set the free-spectral range as 100% and obtained the passband width ratios at −0.5, −1.0, and −3.0 dB, respectively. The ratios are shown in Fig. 5(a) and (b). At −0.5 and −1.0 dB, the passband width ratios are very similar; but at −3.0 dB, the passband width ratio of the RR-MZI becomes greater than that of the RA-MZI

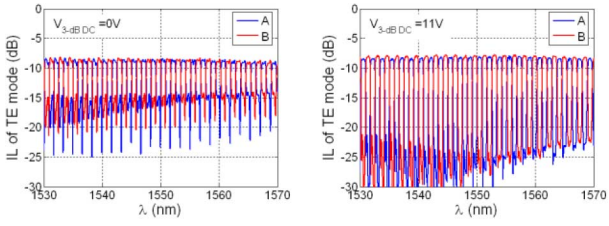

(a) (b)

Fig. 4. Spectra of the RA-MZI interleaver. (a) Spectra of the terminal A and the terminal B waveguides of the RA-MZI with 0 V applied on the 3-dB DC. (b) Spectra of the bar and the cross waveguides of the RA-MZI with 11 V applied.

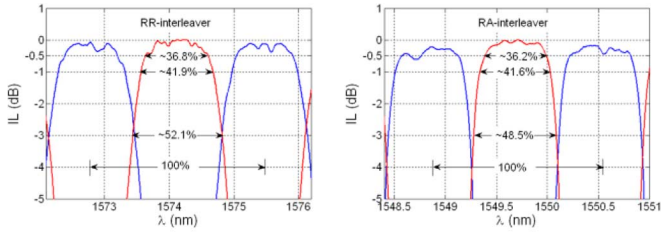

(a) (b)

Fig. 5. Comparison of passbands of the RR- and RA- MZI interleavers in a partial wavelength range. (a) RR-MZI from Fig. 3(b) is applied with 7.5 V. (b) RA-MZI from Fig. 4(b) is applied with 11 V.

structure. As the passband width ratios of the RA-MZI from top to bottom are nearly identical, the RA-MZI structure exhibits more *box*-like passband. However, comparing the entire passband profiles in Figs. 3(b) and 4(b), we can see that the passband peaks of the RR-MZI structure are more uniform, due to the lower propagation loss in the RR-MZI. The perimeter of the RR-MZI structure is shorter than that of the RA-MZI, and the light runs half of the ring only before being coupled into the arm whereas the light in the RA-MZI structure runs a full circle.

IV. Conclusion

We have designed and fabricated RR- and RA-MZI interleaver structures with thermo-optical fine-tuning capability. With thermo-optical tuning, the crosstalk has been improved by $\sim$10 dB. The total IL is ~ -8 dB. Comparing the response spectra of the two structures, we find that the RR-MZI interleaver structure has more uniform passband responses whereas the RA-MZI interleaver structure has sharper rolloffs. Since the responses of both the structures are very sensitive to the outputs of the 3-dB DC, the performances of the interleavers can be improved by replacing the 3-dB DC with a 3-dB multimode interferometer, which is much less wavelength-dependent.

References

[1] S. Cao, J. Chen, J. N. Damask, C. R. Doerr, L. Guiziou, G. Harvey, Y. Hibino, H. Li, S. Suzuki, K. Y. Wu, and P. Xie, "Interleaver technology: Comparisons and applications requirements," in *OFC' 2003 Interleaver Workshop*, pp. 1–9.

[2] H. Arai, H. Nonen, K. Ohira, and T. Chiba, "PLC wavelength splitter for dense WDM transmission system," *Hitachi Cable Rev.*, vol. 21, pp. 11–16, 2002.

[3] S. G. Heris, A. Zarifkar, K. Abedi, and M. K. M. Farshi, "Interleavers/deinterleavers based on Michelson-Gires-Tournois interferometers with different structures," in *Proc. Semiconductor Electronics (ICSE 2004)*, Kuala Lumpur, Malaysia, 2004, vol. 7–9, pp. 573–576.

[4] C. K. Madsen and J. H. Zhao, *Optical Filter Design and Analysis -A Signal Processing Approach*. New York: Wiley, 1999.

[5] B. B. Dingel and M. Izutsu, "Multifunction optical filter with a Michelson–Gires–Tournois interferometer for wavelength-division-multiplexed network system application," *Opt. Lett.*, vol. 23, pp. 1099–1101, 1998.

[6] C. H. Hsieh, R. B. Wang, Z. Q. J. Wen, I. McMichael, P. C. Yeh, C. -W. Lee, and W. H. Cheng, "Flat-top interleavers using two Gires–Tournois etalons as phase-dispersive mirrors in a Michelson interferometer," *IEEE Photon. Technol. Lett.*, vol. 15, no. 2, pp. 242–244, Feb. 2003.

[7] J. Zhang and L. R. L. Zhou, "Novel and simple approach for designing lattice form interleaver filter," *Opt. Express*, vol. 11, pp. 2217–2224, 2003.

[8] C.-W. Lee, R. B. Wang, and P. C. Y.-H. Cheng, "Sagnac interferometer based flat-top birefringent interleaver," *Opt. Express*, vol. 14, pp. 4636–4643, 2006.

[9] Y. Zhang, Q. J. Wang, and T. C. Soh, "Optical Interleaver," U.S. Patent #2005/0271323A1.

[10] Q. J. Wang, Y. Zhang, and Y. C. Soh, "Efficient structure for optical interleavers using superimposed chirped fiber Bragg gratings," *IEEE Photon. Technol. Lett.*, vol. 17, no. 2, pp. 387–389, Feb. 2005.

[11] Q. J. Wang and Y. Z. C. Soh, "All-fiber 3 × 3 interleaver design with flat-top passband," *IEEE Photon.Technol. Lett.*, vol. 16, no. 1, pp. 168–170, Jan. 2004.

[12] K. Jinguji and M. Kawachi, "Synthesis of coherent two-port lattice-form optical delay-line circuit," *J. Lightw. Technol.*, vol. 13, no. 1, pp. 73–82, Jan. 1995.

[13] K. Jinguji, "Synthesis of coherent two-port optical delay-line circuit with ring waveguides," *J. Lightw. Technol.*, vol. 14, no. 8, pp. 1882–1884, Aug. 1996.

[14] M. Oguma, T. Kitoh, K. Jinguji, T. Shibata, and A. H. Hibino, "Passband-width broadening design for WDM filter with lattice-form interleave filter and arrayed-waveguide gratings," *IEEE Photon. Technol. Lett.*, vol. 14, no. 3, pp. 328–330, Mar. 2002.

[15] S. Bidnyk, A. Balakrishnan, A. Delâge, M. Gao, P. A. Krug, P. Muthukumaran, and M. Pearson, "Novel architecture for design of planar lightwave interleavers," *J. Lightw. Technol.*, vol. 23, no. 3, pp. 1435–1440, Mar. 2005.

[16] C. G. H. Roeloffzen, R. M. de Ridder, G. Sengo, K. Wörhoff, and A. Driessen, "Passband flattened interleaver using a Mach-Zehnder interferometer with ring resonator fabricated in SiON waveguide technology," in *Proc. Symp. IEEE/LEOS*, 2002, pp. 32–35.

[17] K. Wörhoff, C. G. H. Roeloffzen, R. M. de Ridder, A. Driessen, and P. V. Lambeck, "Design and application of compact and highly tolerant polatization-independent waveguides," *J. Lightw. Technol.*, vol. 25, no. 5, pp. 1276–1283, May 2007.

[18] Z. P. Wang, S. J. Chang, C. Y. Ni, and Y. J. Chen, "A high-performance ultracompact optical interleaver based on double-ring assisted Mach–Zehnder interferometer," *IEEE Photon. Technol. Lett.*, vol. 19, no. 14, pp. 1072–1074, Jul. 15, 2007.

[19] J. F. Song, Q. Fang, S. H. Tao, M. B. Yu, and G. Q. L. L. Kwong, "Proposed silicon wire interleaver structure," *Opt. Express*, vol. 16, pp. 7849–7859, 2008.

[20] J. F. Song, Q. Fang, S. H. Tao, M. B. Yu, and G. Q. L. L. Kwong, "Passive ring-assisted Mach–Zehnder interleaver on silicon-on-insulator," *Opt. Express*, vol. 16, pp. 8359–8365, 2008.